

DEVELOPMENT WORK FOR A DRABKIN-DEVICE AS A TIME-VARIABLE ANALYZER

G. Badurek¹⁺⁾, A. Kollmar¹, W. Schmatz²

1) Kernforschungsanlage Jülich, SNQ-Projekt, D-5170 Jülich, FRG

2) Kernforschungszentrum Karlsruhe, Institut für Angewandte Kernphysik, D-7500 Karlsruhe, FRG

Abstract

At a pulsed neutron source a new type of inverted geometry time-of-flight spectrometer can be realized by means of a so called Drabkin resonator which is placed between a pair of polarizing supermirrors and thereby acts as an electronically tunable neutron energy analyser. Utilizing a broad incident spectrum scans of constant energy transfer can then readily be performed by proper variation of the resonator transmission function with time according to the different arrival times of neutrons of different energy.

⁺) On leave from Institut für Kernphysik, Technische Universität Wien, A-1020 Wien, Austria

1. Introduction

In polarized neutron scattering experiments one often appreciates the fact that the performance of most spinflip devices used to change the neutron polarization direction with respect to an applied magnetic field depends only weakly, if at all, on neutron energy or wavelength. Spatial spin resonance, first both predicted theoretically and confirmed experimentally by Drabkin and coworkers /1-4/, on the other hand allows to realize a neutron spinflip device with a remarkably pronounced wavelength dependence. When combined with a pair of neutron polarizers such Drabkin spin resonators therefore can serve as neutron monochromators or wavelength analyzers, respectively, whose spectral transmission characteristic can be varied easily by varying the strength of static magnetic fields, i.e. by purely electronic means. It is just this almost instantaneous tunability which makes them suited to conceive a new type of inverted-geometry neutron time-of-flight spectrometer with promising features as proposed recently by Badurek and Schmatz /5/. After a brief explanation of the most essential principles of the spatial neutron spin resonance method we will present in what follows our first conceptual considerations we have begun with in order to build a prototype of such an inverted geometry neutron spectrometer.

2. Principles of spatial spin resonance

As shown schematically in Fig. 1 a Drabkin neutron spin resonator consists of a zig-zag folded conducting foil which generates a static magnetic field \vec{B}_1 of periodically alternating direction orthogonal to that of an additional homogenous field \vec{B}_0 . This resonator system acts much in the same way as a conventional radio-frequency neutron spinflipper, but with the essential difference that each neutron in its own coordinate frame of reference

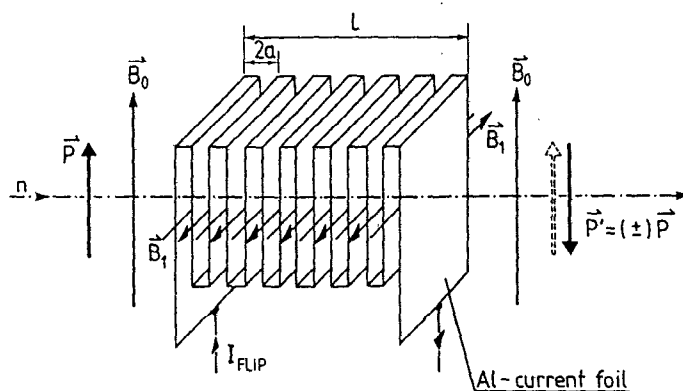


Fig. 1: Schematic arrangement of a magnetic neutron spin resonator.

creates its individual frequency of the transversal field \vec{B}_1

$$\omega = \pi v/a \quad (1)$$

according to its velocity v . There the quantity a is half the period of the spatial oscillations of the conductor foil. The spinflip probability of such a magnetic resonator in close analogy to that of spinflip devices is found as

$$W(v) = \frac{\Gamma^2}{\left(\frac{\delta v}{v_0}\right)^2 + \Gamma^2} \sin^2 \left\{ \frac{\pi l}{2a} \frac{v_0}{v} \sqrt{\left(\frac{\delta v}{v_0}\right)^2 + \Gamma^2} \right\} \quad (2)$$

where l is the active length of the resonator, $\Gamma = 2B_1/\pi B_0$ and

$$v_0 = |\gamma| a B_0 / \pi \quad (3)$$

is that neutron velocity which equals the Larmor frequency $\omega_0 = |\gamma| B_0$ (with $\gamma = -1.83 \times 10^8$ rad/sT). This flipping probability is shown in Fig. 2 as a function of the neutron velocity. Its full-width at half maximum is given as

$$\frac{\delta v_{1/2}}{v_0} \approx 1.59 \frac{a}{l} = \frac{0.8}{N} \quad (4)$$

that means it decreases with increasing number N of resonator oscillations. In defining the quantity Γ of Eq. (2) it is taken into account that only half of the amplitude of the oscillating field \vec{B}_1 , which can be considered as a linear superposition of two fields rotating in opposite directions, effectively contributes to the resonant flipping process. It is furthermore included that according to the Fourier expansion of the "square-wave" resonator field oscillations the first harmonic enters with an relative amplitude $4/\pi$ whereas the influence of higher harmonics has been neglected. Complete flipping takes place at $v = v_0$ if the condition

$$\frac{l}{a} \Gamma = 2k + 1 \quad (k = 0, 1, 2, \dots) \quad (5)$$

is fulfilled. The occurrence of additional sideband maxima in the spinflip

probability vs velocity curve is highly unfavourable, however, for an actual application of the spin resonator as as a neutron monochromator. Two possibilities have been proposed to reduce these unwanted sidebands significantly to a level that can be tolerated.

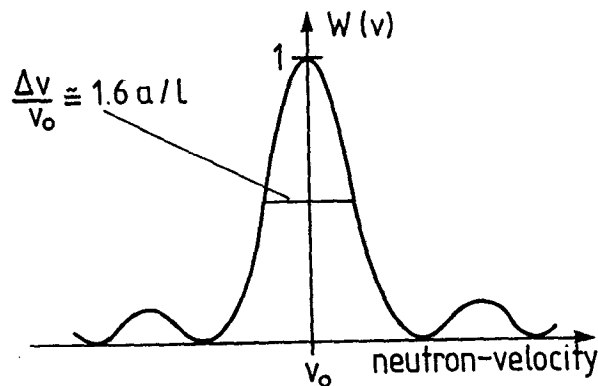


Fig. 2: Velocity dependence of the resonator spinflip probability.

The first method /6/ is based on the use of two successive polarizer-resonator-analyser cascades whose resonators have the same period but different number of oscillations. If the length of the two resonators are matched so that $I/I' = 1.56$, the side maxima of the first cascade happen to coincide with the corresponding minima of the second cascade and hence mutually cancel. Simultaneously the wavelength resolution is improved to

$$\frac{\Delta\lambda}{\lambda} = \frac{\delta v}{v} \frac{1}{2} = 1.37 \frac{a}{l} \quad (6)$$

The signal-to-background ratio is significantly increased too as compared with a single cascade because of the doubled number of polarizing mirror reflections, although the latter is inevitably associated with a decrease of totally transmitted intensity.

The other, conceptually more elegant, method of sideband suppression uses an amplitude modulated transverse field \vec{B}_1 which can be simply achieved by means of a smooth variation of the lateral width of the resonator foil /7/. The functional principle of this method can best be understood if one takes into account that the final reason for the occurrence of sidebands

is the finite duration of the "rf-pulse" the neutrons "see" on their passage through the resonator. This cut-off effect gives rise to sideband components in the frequency spectrum of the rf-pulse which in turn cause spinflip processes of others than the principal frequency ω_0 . As usual in ordinary high-frequency technics the parasitic frequencies are eliminated by proper amplitude modulation of the pulse. Whereas the case of an idealized Drabkin resonator with exponential and Gaussian field amplitude modulation has been treated analytically in ref. /7/ we develop at present a numerical simulation program that can be used to optimize such a resonator under completely realistic conditions as field inhomogenities, finite beam divergency etc. for arbitrary type of modulation /8/.

3. Inverted geometry TOF spectrometer

In a conventional inverted geometry TOF spectrometer only those of the scattered neutrons are allowed to reach the detector whose energy has a preselected fixed value within a given resolution interval. Thus only a small fraction of the incident polychromatic neutron spectrum is actually used if one wants to single out neutrons which have undergone a specific energy transfer upon scattering.

The neutron economy can be much improved, however, if the energy window of the analyser is continuously readjusted according to the different times of arrival at the analyser of neutrons of different initial energy /5/. With an ordinary crystal analyzer this is not possible in practice since it would require a prompt variation of the whole scattering geometry within several milliseconds. With the Drabkin resonator, on the other hand, which can be tuned without any mechanical manipulations simply by changing the currents of the magnet coils and the wiggler such a timevariable energy analyzer can actually be realized. The transmission window of this analyzer can consequently be adjusted properly at any moment so that all scattered neutrons with a certain energy transfer have a chance to reach the detector irrespective of their initial energy before scattering. In order to prove the practical feasibility of this method we are presently installing the experimental arrangement shown schematically in Fig. 3 at one of the new neutron guides of the DIDO reactor at the KFA Jülich.

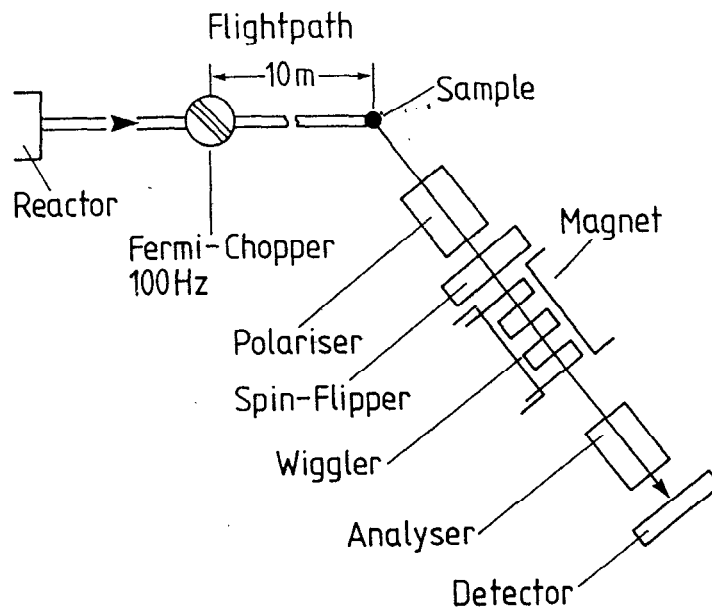


Fig. 3: Sketch of the experimental arrangement.

Since the spectrometer is placed at a continuous neutron source a mechanical chopper is necessary in order to simulate a pulsed source (which would be, of course, the much better choice for such a TOF instrument). The incident flight path from the "source" to the sample is about 10 m. To allow for as much flexibility as possible all components which have to be inserted into the scattered beam path are mounted on an optical bench (total length 2.5 m) that can be rotated around the sample axis. A pair of transversally magnetized supermirror guides /9/ is used as spin polariser and analyser, respectively. Each consists of 60 curved Co-Ti supermirrors /10/ of 30 cm length stacked together with glass distance holders of 1 mm thickness, resulting in a beam cross-section of $30 \times 60 \text{ mm}^2$. The shortest usable neutron wavelength is approximately 2.5 \AA .

A current-sheet spinflipper /11/ is used to achieve a wavelength-independent polarization inversion of the beam by means of sudden field reversal as indicated in Fig. 4. In our arrangement the magnetic field produced by the current-sheet is oriented perpendicular to the guide field, which is only of the order of 0.1 mT at the position where the current-sheet is placed. This arrangement has the advantage that the fields of the polarizer and the analyzer need not to be oriented into opposite directions as was the case with the original current-sheet spinflipper and hence avoids beam depolarization problems in the flipper-"off" state. Our current sheet is made of 0.4 mm thick enamelled copper wires mounted on an aluminium frame in an

arrangement shown in Fig. 5. The wires are parallel across an area of $17 \times 17 \text{ cm}^2$, the maximum current per unit length is about 10 A/mm .

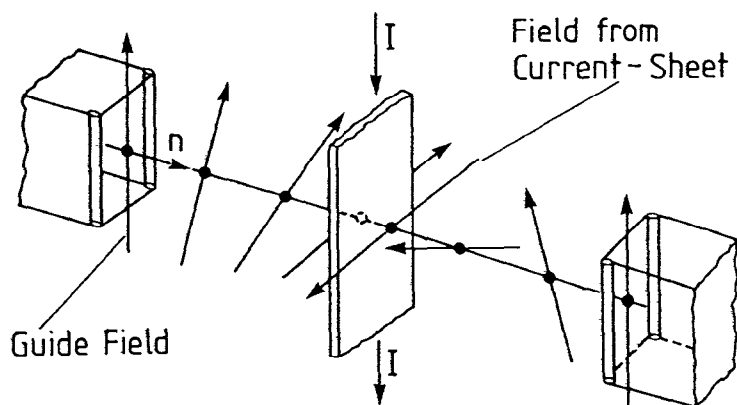


Fig. 4: Sudden field reversal arrangement with a current sheet neutron spinflipper for wavelength-independent polarization inversion.

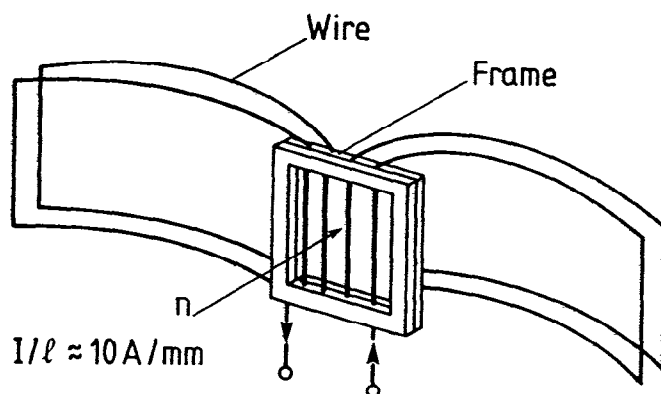


Fig. 5: Schematic sketch of the technical realization of the current sheet spinflipper.

The homogeneous magnetic field \vec{B}_0 of the resonator system is produced by means of an electromagnet shown in Fig. 6. To minimize eddy-current losses the magnet yoke is assembled of many thin iron sheets analogous to the core of electric AC-power transformers. Each of the two magnetizing coils has

30 turns. At the maximum current of 15 A a field of about 20 mT (200 G) is produced within the airgap (height 55 mm) of the magnet. The field homogeneity $\Delta B_0/B_0$ is approximately 1 %.

The spatially alternating field \vec{B}_1 is produced by means of a 0.1 mm thick zigzag-folded aluminium foil. Plastic frames of 2 mm thickness and 50 mm height are used to fix the 55 oscillations of this magnetic wiggler. Its total length is $l = 231$ mm at a period $2a = 4.2$ mm.

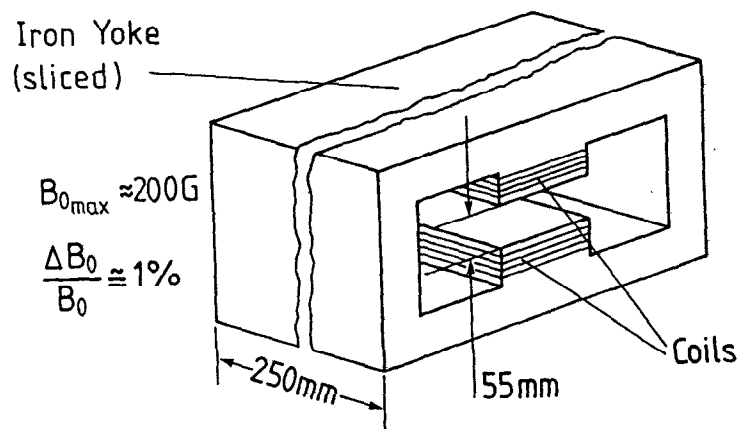


Fig. 6: The electromagnet producing the homogeneous field \vec{B}_0 .

The foil width w (which is chosen to be constant in our first prototype arrangement) is 75 mm. The beam window of the plastic frames has the dimensions 55×30 mm². Calculations of \vec{B}_1 according to Biot-Savart's law of electrodynamics yields the relation

$$B_1 \approx \frac{\mu_0}{2} \frac{I_1}{w} \quad (7)$$

between the amplitude of the field and the foil current I_1 . $\mu_0 = 4\pi \times 10^{-7}$ Vs/Am is the vacuum permeability. From Eq. (5) then follows the current which is necessary for complete polarization reversal

$$I_1^{flip} = (2k + 1) \frac{\pi^2 w v_0}{\mu_0 |\gamma| \Gamma} \quad k = 0, 1, 2, \dots \quad (8)$$

At $\lambda = 2.5 \text{ \AA}$ ($v_0 = 1580 \text{ m/s}$) first order ($k = 0$) spinflip requires hence in our case a current $I_1 = 22 \text{ A}$, corresponding to a field $B_1 = 0.18 \text{ mT}$ (1.8G). By means of several clamping connections at every 5th period the active length of our resonator and hence its wavelength resolution can be varied between the limits

$$1.4 \times 10^{-2} \leq \frac{\Delta\lambda}{\lambda} \leq 5.5 \times 10^{-2} \quad (9)$$

if one takes into account the associated change of the flip current according to Eq. (8). However, not all of this resolution range is accessible in the dynamic mode of operation of the resonator with our spectrometer geometry, as will be pointed out later (see Eqs. 12 and 13).

In an inverted geomtry TOF spectrometer the energy transfer of the neutrons upon scattering of the sample is found from the relation

$$\Delta E = \frac{m}{2} \left\{ \frac{L_I^2}{(t - L_F/v_0)^2} - v_0^2 \right\} \quad (10)$$

where m is the neutron mass, t the total neutron time-of-flight, v_0 the velocity which is transmitted by the analyzer and where L_I and L_F denote the distances from the source to the sample and from the sample to the detector, respectively. If the resonance analyzer is placed immediately behind the sample and if its active length is negligible as compared to the other flight path distances, a scan at constant energy transfer ΔE can be performed by varying the field \vec{B}_0 of the resonator with time according to /5/

$$B_0(t_I) = \frac{\pi L_I}{|\gamma| a t_I} \left\{ 1 - \frac{2\Delta E}{m} \left(\frac{t_I}{L_I} \right)^2 \right\}^{1/2} \quad (11)$$

where $L_I/v_{\max} < t_I < L_I/v_{\min}$ is the neutron time-of-flight along the primary path L_I . The velocity limits v_{\min} and v_{\max} belong the longest and shortest wavelengths in the incident neutron spectrum. An analogous time-dependence is required for the amplitude of the oscillating field. Fig. 7 shows schematically how the fields are varied during the measurement. At each source pulse (repetition frequency 100 Hz) the fields start with a maximum value

and then decrease gradually with time according to Eq. (11), which in case of elastic scattering ($\Delta E = 0$) yields a simple $1/t$ -dependence. At the end of each pulse cycle both fields are raised again to their initial value. As indicated too in Fig. 7

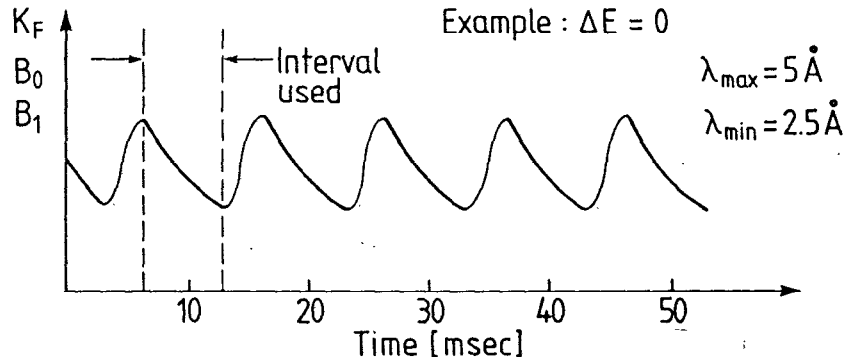


Fig. 7: Time-dependence of the fields \vec{B}_0 and \vec{B}_1 of the magnetic resonator for elastic scattering. Both fields decrease inversely with time synchronously with the repeated source pulses.

the wavenumber $k_f(t)$ of the scattered neutrons which are transmitted by this resonant analyzer consequently varies too, so that a certain energy transfer $\Delta E \propto k_I^2(t) - k_f^2(t)$ is measured with many pairs $k_I - k_f$ simultaneously.

For a proper operation of such a spectrometer one has to take care, however, that the fields vary slowly enough with time to consider them as being constant and the resonance condition $v = v_0$ being fulfilled during the neutron transmission time interval $\Delta t = 1/v$ through the resonator. This condition requires the fulfilment of the relation

$$\left| \frac{dv_0}{dt} \right| \Delta t < \frac{\delta v_{1/2}}{2} \quad (12)$$

which in turn leads to

$$\frac{\Delta t}{t} \cdot \frac{1}{a} = \frac{1^2}{L a} < 0.8 \quad (13)$$

where L is the distance from the chopper to the resonator and t the corresponding neutron time-of-flight for that distance. In our case with $L \approx 10$ m this means that the usable active length of our resonator is restricted to $l < 130$ mm or a wavelength resolution $\Delta\lambda/\lambda > 2.6 \times 10^{-2}$. Making use of its full resolution capability in the dynamic application would require an increase of the distance L to about 32 m.

References

- /1/ G.M. Drabkin, Sov. Phys. JETP 16 (1963) 281
- /2/ G.M. Drabkin, V.A. Trunov and V.V. Runov, *ibid* 27 (1968) 194
- /3/ G.M. Drabkin, V.A. Ruban and V. I. Sbitnev, Sov. Phys. Techn. Phys. 17 (1972) 855
- /4/ M.M. Agamalian, G.M. Drabkin and V.T. Lebedev, Sov. Phys. JETP 46 (1977) 200
- /5/ G. Badurek and W. Schmatz, Proc. Int. Conf. "Neutron Scattering in the Nineties", Jülich 1985 (IAEA-CN46/85 Vienna 1985) p. 77
- /6/ M.M. Agamalian, J. Schweitzer, Ya.M. Otchik and V.P. Khavronin, Nucl. Instr. Meth. 158 (1979) 395
- /7/ M.M. Agamalian and V.V. Deriglazov, Sov. Phys. JETP 56 (1982) 166
- /8/ G. Badurek, W. Neuhaus and A. Kollmar, to be published in Nucl. Instr. Meth.
- /9/ O. Schärpf, in Neutron Scattering 1981 (J. Faber, Ed.), Proc. AIP Conf. No. 89 (Argonne Nat. Lab.), Am. Inst. Phys. (1982) 182
- /10/ F. Mezei and P. Dagleish, Comm. Phys. 1 (1976) 81 and 2 (1977) 41
- /11/ A. Abrahams, O. Steinsvoll, P.J.M. Bongarts and P.W. de Lange, Rev. Sci. Instr. 33 (1962) 524.